Model of Strong Ground Motions from Earthquakes in Central and Eastern North America: Best Estimates and Uncertainties

Gabriel R. Toro
Risk Engineering, Inc.

Norman A. Abrahamson
Pacific Gas and Electric Company

John F. Schneider
Impact Forecasting

ABSTRACT

Ground-motion attenuation equations for rock sites in central and eastern North America are derived, based on the predictions of a stochastic ground-motion model. Four sets of attenuation equations are developed (*i.e.*, 2 crustal regions × 2 magnitude scales). The associated uncertainties are derived by considering the uncertainties in parameter values, as well as those uncertainties associated with the ground-motion model itself. Comparison to data shows a reasonable agreement. Comparison to other attenuation functions for the region shows consistency with most attenuation functions in current use.

INTRODUCTION

This paper presents a set of attenuation equations for spectral acceleration (SA) and peak ground acceleration (PGA) in central and eastern North America (CENA), based on a stochastic model of source excitation and a model of path effects that considers multiple rays in a horizontally layered model of the crust. These models and the values of their parameters were developed following an extensive analysis of ground-motion data and other relevant data. This effort is documented in EPRI (1993) and in a series of upcoming papers (Schneider *et al.*, 1996; Abrahamson *et al.*, 1996a, 1996b). The objective in the EPRI study was to obtain both the best-estimate value and the associated uncertainty in each parameter, and to carry these uncertainties through to the final results. This paper presents the best estimates and uncertainties in the ground motions predicted by the stochastic model, in a functional form that is amenable to use in probabilistic hazard analysis and other earthquake-engineering applications, as well as some insights developed from these results and comparisons to other attenuation equations that have been proposed for CENA. Additional information about the derivation of these attenuation equations is provided in EPRI (1993) and Toro *et al.* (1996).

The frequency band, distance range, and magnitude range of interest for this study are 1 to 35 Hz, 1 to 500 km (with emphasis on distances of 1 to 100 km), and moment magnitude 5 to 8. Separate attenuation equations are obtained for two crustal regions found to be typical of CENA, for each of six frequencies and for peak ground acceleration, and for two different magnitude scales (*i.e.*, moment magnitude M and Lg-wave magnitude m_{Lg}). The results presented here are directly applicable to hard rock (defined as having average shear-wave velocities of 6,000 ft/s at the surface). Results for soil sites may be obtained from these results by using the amplification factors in EPRI (1993) and Silva *et al.* (1996).

Other studies (*e.g.*, Atkinson, 1984; Boore and Atkinson, 1987; Toro and McGuire, 1987; McGuire *et al.*, 1988; Atkinson and Boore, 1995) have used a similar stochastic model to derive attenuation equations for CENA. This study is the first to develop a comprehensive quantification of the uncertainties in model parameters for CENA ground motions and to propagate these uncertainties to obtain the total uncertainty in ground-motion amplitude.

This paper begins with a summary of the stochastic ground-motion model, the parameters used to represent source and path effects in the study region, and the uncertainties in these parameters. This summary is not exhaustive and the reader is referred to EPRI (1993), Schneider *et al.* (1996), and Abrahamson *et al.* (1996a, 1996b) for further details on the model or its justification. This summary is followed by the tables and equations that describe attenuation functions and associated measures of uncertainty. Next, this

paper presents comparisons to data and to other attenuation equations proposed for CENA. Finally, this paper describes the procedure for estimating ground-motion at soil sites.

SUMMARY OF MODEL, PARAMETERS, AND UNCERTAINTIES

The stochastic model of earthquake ground motions uses simplified, yet physically based, representations of seismic energy release and wave propagation to obtain predictions of ground-motion amplitude for given values of earthquake size and depth, distance to the site, and model parameters. The source excitation is characterized by means of Brune's ω-squared model (Brune, 1970, 1971). The model for geometric attenuation considers the effect of crustal structure by using the formulation of Ou and Herrmann (1991; refinements to this formulation are documented in EPRI, 1993). The model for anelastic attenuation considers both crustal and near-surface attenuation (by means of parameters $Q(f)$ and kappa, respectively). A comprehensive test of the stochastic model against recorded motions for several large magnitude events is contained in EPRI (1993) and Schneider *et al.* (1996). This test shows that the stochastic model is consistent with the recorded ground motions for the frequency, distance, and magnitude range of interest (*i.e.*, the bias in the model predictions is essentially zero for most frequencies, considering its statistical uncertainty).

The key parameters for the stochastic model are stress-drop, crustal velocity structure, crustal anelastic attenuation (Q), near-site anelastic attenuation (κ or kappa), and focal depth. The selected values and associated uncertainties for these parameters are described below, after the definition of some terms related to uncertainty.

Types of Uncertainties

It is customary in seismic hazard studies to distinguish between two types of uncertainty, as follows:

Epistemic Uncertainty. Uncertainty that is due to incomplete knowledge and data about the physics of the earthquake process. In principle, epistemic uncertainty can be reduced by the collection of additional information.

Aleatory Uncertainty. Uncertainty that is inherent to the unpredictable nature of future events. It represents unique details of source, path, and site response that cannot be quantified before the earthquake occurs. Aleatory uncertainty cannot be reduced by collection of additional information. One may be able, however, to obtain better estimates of the aleatory uncertainty by using additional data.

This paper will refer to the combined epistemic and aleatory uncertainty as total uncertainty (or simply uncertainty). Epistemic and aleatory uncertainty are sometimes called "Uncertainty" and "Randomness," respectively.

To bring these concepts into the context of ground-motion prediction, consider that ground-motion models give estimates of the probability distribution of ground-motion amplitude for a given event. For most ground-motion models, including the one presented here, this distribution is assumed to be lognormal and is characterized by a median (μ) and a logarithmic standard deviation (σ). The scatter quantified by σ is the aleatory uncertainty.

Due to the limited data available, there is epistemic uncertainty in the values of μ and σ for a given magnitude and distance. This epistemic uncertainty is denoted σ_μ and σ_σ. The values of these quantities may be magnitude- and distance-dependent.

From the point of view of the ground-motion analyst or modeler, the total uncertainty in predicted ground motions is often partitioned in a manner that may be considered orthogonal to the above partition (see Abrahamson *et al.*, 1990), as follows:

Modeling Uncertainty. Represents differences between the actual physical process that generates the strong earthquake ground motions and the simplified model used to predict ground motions (Abrahamson *et al.*, 1990, call this modeling+random uncertainty). Modeling uncertainty is estimated by comparing model predictions to actual, observed ground motions. Because it is computed from comparisons to data, the modeling uncertainty captures all shortcomings of the model (provided that a sufficient number of earthquakes with a wide distribution of magnitudes and distances are used to estimate the modeling uncertainty).

Parametric Uncertainty. Represents uncertainty in the values of the model's event, path, and site-specific parameters (*e.g.*, stress drop) for future earthquakes. Parametric uncertainty is quantified by observing the variation in parameters inferred (usually in an indirect manner) for several earthquakes and/or several recordings.

It is important to recognize that the distinction between modeling and parametric uncertainty is model-dependent. For instance, one may reduce the scatter in the predictions by making the model more complete, thereby introducing new parameters in the model. Unless these new parameters are known a priori for future earthquakes and for the site of interest, there will be additional parametric uncertainty, thereby transferring some modeling uncertainty into parametric uncertainty, without varying the total uncertainty (at least for the types of events and sites that are well represented in the data).

Both the modeling and parametric uncertainties contain epistemic and aleatory uncertainty. For instance, observed scatter that is not accounted for by the model and varies from event to event is aleatory modeling uncertainty, whereas statistical uncertainty about the bias of the model's median estimate (due to limited data) is epistemic modeling uncertainty. Similarly, the event-to-event variation in stress

TABLE 1.
Partition of Uncertainty in Ground-Motion Prediction

		Seismic-Hazard Analyst	
		Epistemic (σ_μ,σ_σ)	**Aleatory (σ)**
Ground-Motion Analyst	**Modeling**	σ_μ: Uncertainty in the true bias of model σ_σ: Uncertainty in estimate of $\sigma_{modeling}$	$\sigma_{modeling}$: Unexplained scatter due to physical processes not included in the model
	Parametric	σ_μ: Uncertainty in median values of source, path, and site parameters σ_σ: Uncertainty in probability distributions of source, path, and site parameters	σ_{param}: Event-to-event variation in source, path, and site-specific parameters of the model

drop is aleatory parametric uncertainty, whereas the imperfect knowledge about the probability distribution of stress drops from future earthquakes (*e.g.*, What is the median stress drop for *M* 7 earthquakes?) is epistemic parametric uncertainty. Table 1 illustrates this two-way partition of total uncertainty.

The distinctions among the various types of uncertainty are subtle, but important in practice. They determine whether a particular component of uncertainty affects the median hazard curve or the associated uncertainty band. They also affect how the observed squared residuals are partitioned. The most important reason for these distinctions is, however, to make sure that all uncertainties in the various pieces of the ground-motion model are considered, in order to obtain a realistic estimate of the total uncertainty.

Model Parameters and their Uncertainties

Stress Drop. The stress drop is a key parameter in the Brune model of source excitation: it determines how the corner frequency, the Fourier amplitude at high frequencies, and the source duration vary as a function of seismic moment. The median stress drop (120 bars) and its uncertainty were determined from the CENA stress-drop compilation of Atkinson (1993), adjusted to make the stress-drop values consistent with the crustal shear-wave velocity used in the EPRI study (see Figure 1a). Stress drops obtained in the EPRI study by inversion of seismograph data from CENA (see EPRI, 1993, or Abrahamson, 1996a) yield similar results.

The data for large magnitudes are sparse, but they suggest a reduction in the median stress drop and in the scatter with increasing magnitude (Figure 1a). This study conservatively ignored this possible reduction in median for large magnitudes, but increased the epistemic uncertainty in the median stress drop (*i.e.*, increasing σ_μ) for large magnitudes.

The aleatory uncertainty in stress drop was assumed to be smaller for larger magnitudes. This is consistent with empirical studies that show a reduction in σ (*i.e.*, the total aleatory uncertainty in ground-motion amplitude) for larger magnitudes (*e.g.*, Youngs *et al.*, 1995). The resulting model for the epistemic and aleatory uncertainties in stress drop is shown in Figure 1b. Note that the total uncertainty in stress drop is assumed to be constant, but its partition into epistemic and aleatory is magnitude-dependent.

Focal Depth. Initially, separate probability distributions were constructed for rifted and non-rifted CENA areas, but these differences do not lead to statistically significant differences in predicted ground motions. Thus, we use a single probability distribution of focal depth for all of CENA (see EPRI, 1993, and Abrahamson *et al.*, 1996b). Uncertainty in focal depth is treated as being all aleatory; epistemic uncertainty in depth is not considered.

Crustal Velocity Structure. Sixteen crustal velocity models were compiled for the various tectonic domains in CENA (see Figure 2), and the effects of these velocity models on ground-motion amplitude were evaluated. We determined that—for the purposes of ground-motion calculations for the depth, distance, and frequency range of interest—15 of the 16 crustal models predicted similar ground motions and could be grouped into one (see EPRI, 1993, or Abrahamson *et al.*, 1996b). Based on this result, the CENA is partitioned into two attenuation regions, namely the Gulf Coastal Plain (region 4) and everything else (represented by the crustal structure in region 12: the Midcontinent region). These representative crustal structures are then used in separate simulations that we use to derive the engineering model for each region. Uncertainty in crustal structure (within each attenuation region) is not modeled explicitly as parametric uncertainty. This uncertainty is, however, included in the modeling uncertainty obtained from comparisons of data to predictions (EPRI, 1993; Schneider *et al.*, 1996).

Near-Site Anelastic Attenuation, Kappa. The analysis of data on kappa for CENA and the western United States (WUS) is described in EPRI (1993) and Abrahamson *et al.* (1996b). A kappa of 0.006 provides an adequate match to the spectral shape of CENA hard rock ground motions. Uncertainty in the larger dataset of WUS kappa values for rock is described

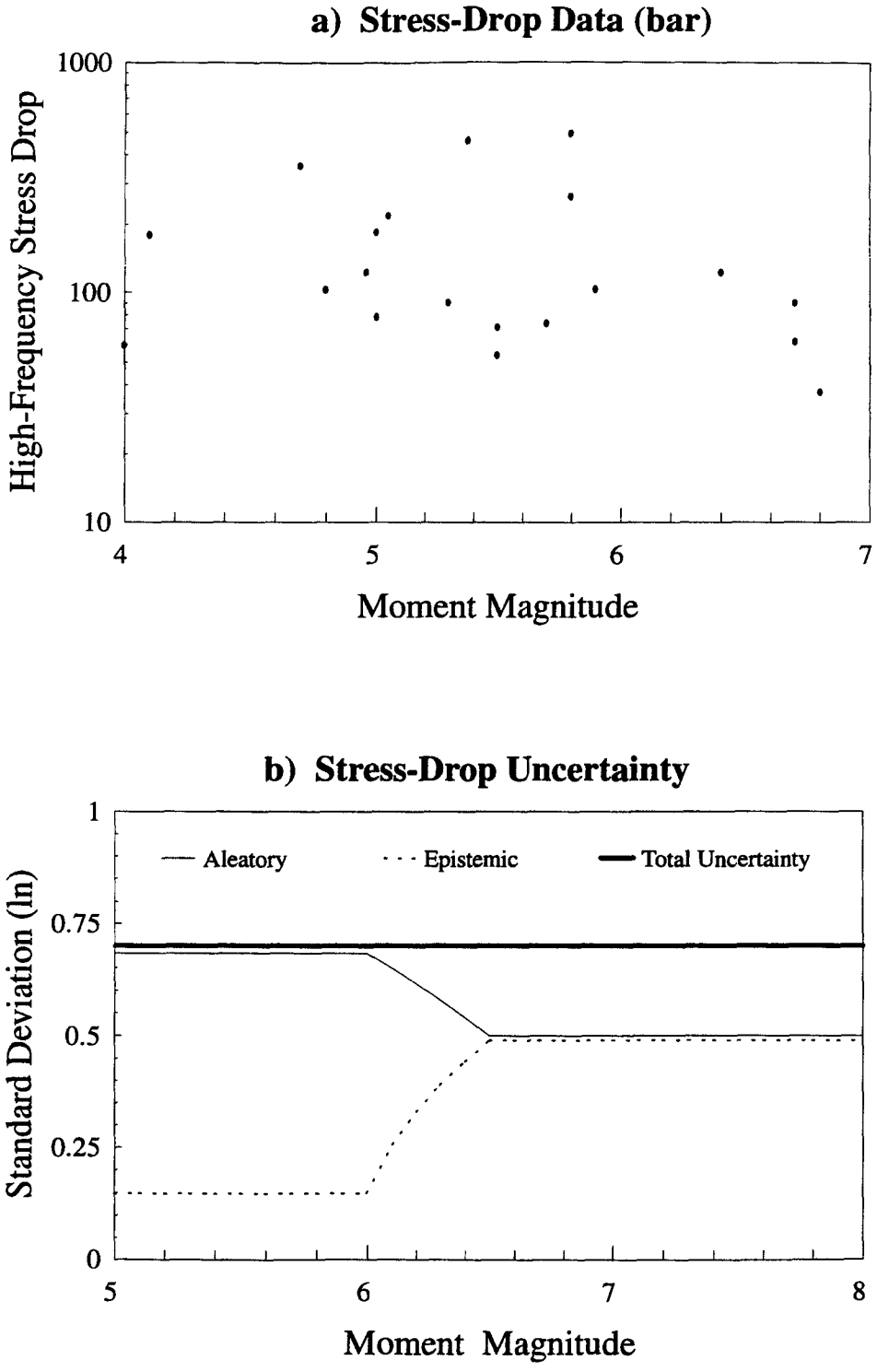

▲ **Figure 1.** a) Stress-drop data (adjusted from Atkinson, 1993). b) Model of stress-drop uncertainty. Note: The total uncertainty (expressed as a standard deviation) is equal to the square root of the sum of the squares of the epistemic and aleatory uncertainties.

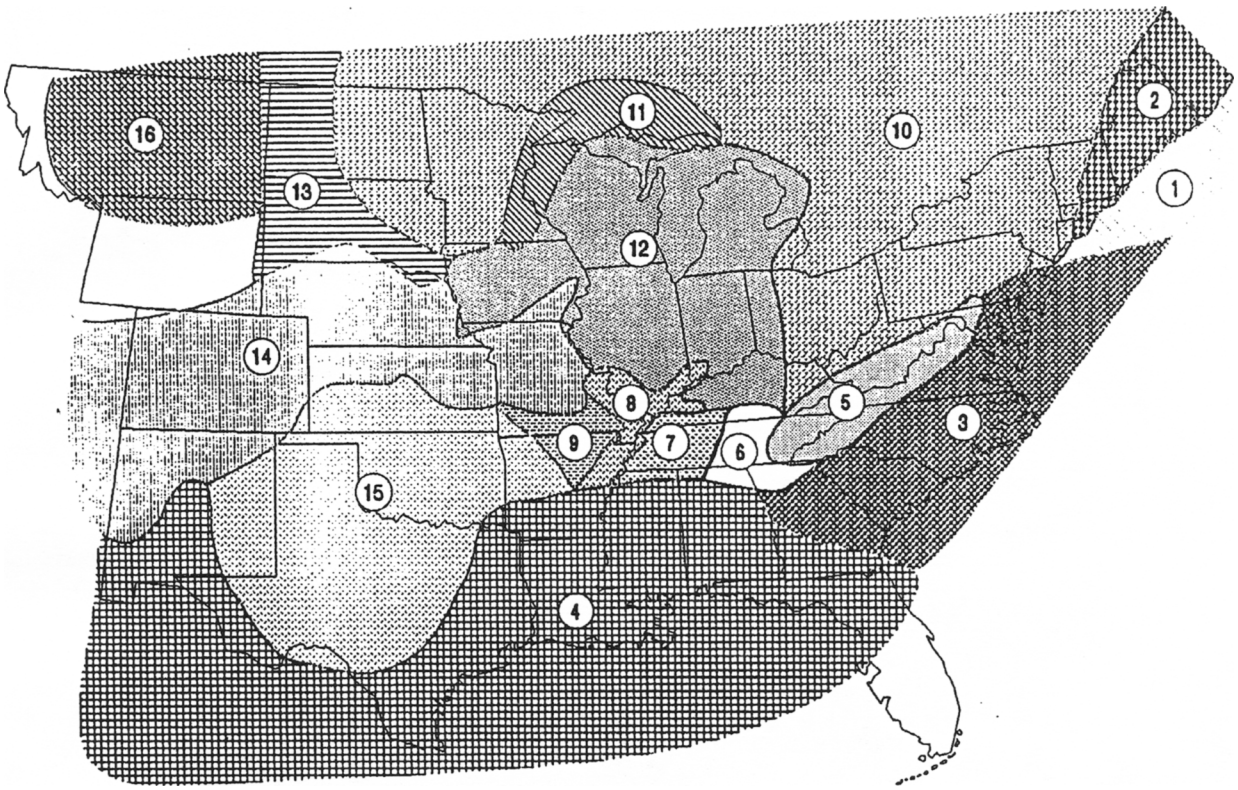

▲ **Figure 2.** Regionalization of crustal structure for CENA. Attenuation equations are developed for the Mid-continent and Gulf crustal regions (regions 12 and 4, respectively). The equations for the Mid-continent are applicable to regions 1 through 3 and 5 through 16.

as log-normally distributed with a logarithmic standard deviation of 0.4. This study used three equally weighted values of 0.003, 0.006, and 0.012, which correspond to a logarithmic standard deviation of 0.7.

Epistemic uncertainty in kappa was neglected in this study. It should be noted, however, that to the extent that kappa is a property of each individual site (for which one can obtain better estimates using site-specific geophysical measurements or recordings), some of its uncertainty should be considered epistemic. The same is true for variations in near-surface shear-wave velocities among rock sites. This study treats variations within a region as aleatory uncertainty, as is common practice.

Crustal Anelastic Attenuation, Q. The data on Q for the two attenuation regions are described in EPRI (1993) and Abrahamson *et al.* (1996b). The uncertainty in Q for each region is characterized by three models that are given equal weights based on the EPRI (1993) analyses and on earlier studies. This uncertainty is considered all aleatory, as it is thought that most of this uncertainty is due to regional variations in crustal properties. Again, if one considers a smaller region around a specific site, some of the uncertainty in Q should be treated as epistemic.

Modeling Uncertainty

The modeling uncertainty is determined from the misfit of modeled ground motion data with recorded data, as described in EPRI (1993) and Schneider *et al.* (1996). The epistemic modeling uncertainty is made up of the site-correction terms (called D terms in the above references) and the model bias. The aleatory modeling uncertainty is made up of the remaining misfit or scatter (allowing the D terms to be different from 1). The resulting modeling uncertainties are approximated by

$$\sigma_{a,\text{modeling}} = \begin{cases} 0.32 & f > 9\text{Hz} \\ 0.63 - 0.14\ln(f) & 2 < f \le 9\text{Hz} \\ 0.53 & f \le 2\text{Hz} \end{cases} \quad (1)$$

$$\sigma_{e,\text{modeling}} = 0.27 \quad (2)$$

where σ represents standard deviation in natural log units.

Total Uncertainty

In summary, aleatory uncertainty in the predicted ground motions comes from parametric uncertainty in stress drop,

focal depth, kappa and Q, and from aleatory modeling uncertainty. Epistemic uncertainty in the predicted ground motions comes from epistemic parametric uncertainty in stress drop and from epistemic modeling uncertainty.

FUNCTIONAL FORM OF PREDICTIVE EQUATIONS

Practical considerations dictate that the ground-motion predictions for engineering applications must be in the form of relatively simple equations in terms of magnitude and distance (we will call this set of attenuation functions the Engineering Model). The functional form and number of terms in these equations must, however, be sufficient to match the main features of the ground motions predicted by the stochastic ground-motion model described earlier over the entire range of magnitudes, distances, and frequencies of engineering interest.

The functional form adopted here is the following:

$$\ln Y = C_1 + C_2(M-6) + C_3(M-6)^2 - C_4 \ln R_M - (C_5 - C_4)\max\left[\ln\left(\frac{R_M}{100}\right), 0\right] - C_6 R_M + \varepsilon_e + \varepsilon_a \quad (3)$$

$$R_M = \sqrt{R_{jb}^2 + C_7^2} \quad (4)$$

where Y is spectral acceleration or peak ground acceleration (in units of g), C_1 through C_7 are constants to be determined from the modeling results (see next section), M is either Lg magnitude (m_{Lg}) or moment magnitude (M), and R_{jb} is the closest *horizontal* distance (or Joyner-Boore distance) to the earthquake rupture (km).

The quadratic magnitude term is needed in order to provide a better fit to the model predictions for low-frequency ground motions (it is not required for frequencies of 5 Hz or higher). The magnitude terms are of the form $(M-6)^n$ for the sake of numerical stability in the values of C_2 and C_3. The terms in C_4 and C_5 represent geometrical spreading with slopes (in log-log space) C_4 (R_M < 100 km) and C_5 (R_M > 100 km). The model with two slopes provides a better fit to the crustal effects predicted by the ground-motion model in Schneider *et al.* (1996).

Uncertainty in ground-motion amplitude is represented by the quantities ε_a (aleatory) and ε_e (epistemic), which are assumed to follow normal distributions with mean zero. The standard deviations of ε_a and ε_e are, in general, dependent on magnitude and distance.

Table 2 lists the values of coefficients C_1 through C_7. Separate sets of coefficients are provided for the Midcontinent* and Gulf crustal models and for the two choices of magnitude variable.

*We refer to the midcontinent as a "region," although it is a group of crustal regions.

Figures 3 and 4 show representative predictions by the Engineering Model for the two representative crustal regions and for the two magnitude representations considered in this study. Comparing the predictions for the two regions, we observe that ground motions at short distances are higher for the Gulf region due to lower shear-wave velocities (which produce greater amplification) near the surface. At longer distances, this effect is counteracted by higher anelastic attenuation in the Gulf region, resulting in lower predictions.

Figures 3 and 4 indicate only a minor discontinuity in slope at 100 km as a result of crustal reflections. Discontinuities introduced by the layered crustal structure are smoothed out by the distribution of hypocentral depth. These discontinuities increase uncertainty near 100 km, as will be shown in Figure 5.

QUANTIFICATION OF UNCERTAINTY

The combined effect of all parametric uncertainties is obtained by performing statistics on the residuals from the least-squares fit to model predictions. The modeling uncertainty is added later.

Figure 5 (panels a and b) illustrates the various components of aleatory uncertainty and their dependence on distance for M 6.5 in the Midcontinent. This figure shows that depth is a very important contributor to aleatory uncertainty at short distances, stress drop and modeling error are important contributors at all distances, and Q is an important contributor at long distances (particularly for high frequencies). Figure 5 (panels c and d) shows the components of aleatory uncertainty and their dependence on moment magnitude for a distance of 20 km.

Figure 6 shows the components of epistemic uncertainty and their dependence on magnitude for a distance of 20 km, and for attenuation equations in terms of both M and m_{Lg} (Figure 6 also shows the total uncertainty). Epistemic uncertainty is higher, and aleatory uncertainty is slightly lower, for higher magnitudes. This is a consequence of our assumption about the magnitude dependence of the epistemic and aleatory uncertainties in stress drop (see Figure 1 and Equation 1). Aleatory uncertainty is higher for low-frequency ground motions due to higher aleatory modeling uncertainty.

The equations and tables that follow provide a simplified representation of how the aleatory and epistemic uncertainties vary as a function of magnitude and distance for the various ground-motion measures. The emphasis here is on the magnitude-distance-frequency combinations of engineering interest. Little attention is paid to unimportant combinations such as high frequencies at long distances.

The expressions for the total aleatory uncertainty in ground-motion amplitude for a given magnitude and distance can be decomposed into a magnitude-dependent term (aleatory modeling uncertainty plus aleatory uncertainty due to stress drop) and a distance-dependent term (aleatory uncertainty due to focal depth, Q, and kappa). Thus, the total aleatory uncertainty is given by the following equation:

TABLE 2
Coefficients of Attenuation Equations

Freq. (Hz)	Median		Weight=0.046		Weight=0.454		Weight=0.454		Weight=0.046		Median and all cases				
	C_1	C_2	C_1	C_2	C_1	C_2	C_1	C_2	C_1	C_2	C_3	C_4	C_5	C_6	C_7
Midcontinent, equations using Moment Magnitude															
0.5	−0.74	1.86	−1.53	1.72	−0.99	1.82	−0.49	1.91	0.05	2.00	−0.31	0.92	0.46	0.0017	6.9
1	0.09	1.42	−0.75	1.25	−0.18	1.36	0.35	1.47	0.93	1.58	−0.20	0.90	0.49	0.0023	6.8
2.5	1.07	1.05	0.23	0.89	0.81	1.00	1.34	1.10	1.91	1.21	−0.10	0.93	0.56	0.0033	7.1
5	1.73	0.84	0.89	0.68	1.46	0.79	1.99	0.89	2.57	1.00	0.00	0.98	0.66	0.0042	7.5
10	2.37	0.81	1.53	0.65	2.10	0.76	2.64	0.86	3.21	0.97	0.00	1.10	1.02	0.0040	8.3
25	3.68	0.80	2.84	0.63	3.41	0.74	3.95	0.85	4.52	0.96	0.00	1.46	1.77	0.0013	10.5
35	4.00	0.79	3.16	0.63	3.74	0.74	4.27	0.85	4.84	0.96	0.00	1.57	1.83	0.0008	11.1
PGA	2.20	0.81	1.36	0.64	1.93	0.75	2.46	0.86	3.04	0.97	0.00	1.27	1.16	0.0021	9.3
Midcontinent, equations using Lg Magnitude															
0.5	−0.97	2.52	−1.83	2.29	−1.24	2.45	−0.69	2.60	−0.10	2.76	−0.47	0.93	0.6	0.0012	7.0
1	−0.12	2.05	−0.94	1.86	−0.38	1.99	0.14	2.11	0.70	2.23	−0.34	0.90	0.59	0.0019	6.8
2.5	0.90	1.70	0.10	1.53	0.64	1.64	1.15	1.75	1.69	1.86	−0.26	0.94	0.65	0.0030	7.2
5	1.60	1.24	0.80	1.07	1.35	1.18	1.85	1.29	2.39	1.40	0.00	0.98	0.74	0.0039	7.5
10	2.36	1.23	1.57	1.07	2.11	1.18	2.62	1.28	3.16	1.39	0.00	1.12	1.05	0.0043	8.5
25	3.54	1.19	2.75	1.03	3.29	1.14	3.79	1.24	4.34	1.35	0.00	1.46	1.84	0.0010	10.5
35	3.87	1.19	3.08	1.03	3.62	1.14	4.12	1.24	4.66	1.35	0.00	1.58	1.9	0.0005	11.1
PGA	2.07	1.20	1.27	1.04	1.81	1.15	2.32	1.25	2.86	1.36	0.00	1.28	1.23	0.0018	9.3
Gulf, equations using Moment Magnitude															
0.5	−0.81	1.72	−1.6	1.58	−1.06	1.67	−0.56	1.76	−0.02	1.86	−0.26	0.74	0.71	0.0025	6.6
1	0.24	1.31	−0.6	1.15	−0.03	1.26	0.51	1.36	1.08	1.48	−0.15	0.79	0.82	0.0034	7.2
2.5	1.64	1.06	0.80	0.90	1.38	1.01	1.91	1.12	2.48	1.23	−0.08	0.99	1.27	0.0036	8.9
5	3.10	0.92	2.26	0.76	2.83	0.87	3.36	0.97	3.94	1.08	0.00	1.34	1.95	0.0017	11.4
10	5.08	1.00	4.25	0.84	4.82	0.95	5.35	1.05	5.92	1.16	0.00	1.87	2.52	0.0002	14.1
25	5.19	0.91	4.35	0.74	4.92	0.86	5.46	0.96	6.03	1.07	0.00	1.96	1.96	0.0004	12.9
35	4.81	0.91	3.97	0.74	4.54	0.86	5.08	0.96	5.65	1.07	0.00	1.89	1.8	0.0008	11.9
PGA	2.91	0.92	2.07	0.75	2.64	0.86	3.18	0.97	3.75	1.08	0.00	1.49	1.61	0.0014	10.9
Gulf, equations using Lg Magnitude															
0.5	−1.01	2.38	−1.87	2.14	−1.28	2.30	−0.73	2.45	−0.15	2.61	−0.42	0.75	0.83	0.0032	6.8
1	0.06	1.97	−0.76	1.78	−0.2	1.91	0.32	2.03	0.88	2.16	−0.32	0.8	0.92	0.0030	7.3
2.5	1.49	1.74	0.69	1.57	1.23	1.68	1.74	1.79	2.28	1.90	−0.26	1	1.36	0.0032	9.0
5	3.00	1.31	2.20	1.15	2.74	1.26	3.25	1.36	3.79	1.47	0.00	1.35	2.03	0.0014	11.4
10	4.65	1.30	3.86	1.14	4.40	1.25	4.91	1.35	5.45	1.46	0.00	1.78	2.41	0.0000	13.8
25	5.08	1.29	4.29	1.13	4.83	1.24	5.33	1.34	5.87	1.45	0.00	1.97	2.04	0.0000	12.9
35	4.68	1.30	3.88	1.13	4.42	1.24	4.93	1.35	5.47	1.46	0.00	1.89	1.88	0.0005	11.9
PGA	2.80	1.31	2.00	1.14	2.54	1.25	3.05	1.36	3.59	1.47	0.00	1.49	1.68	0.0017	10.9

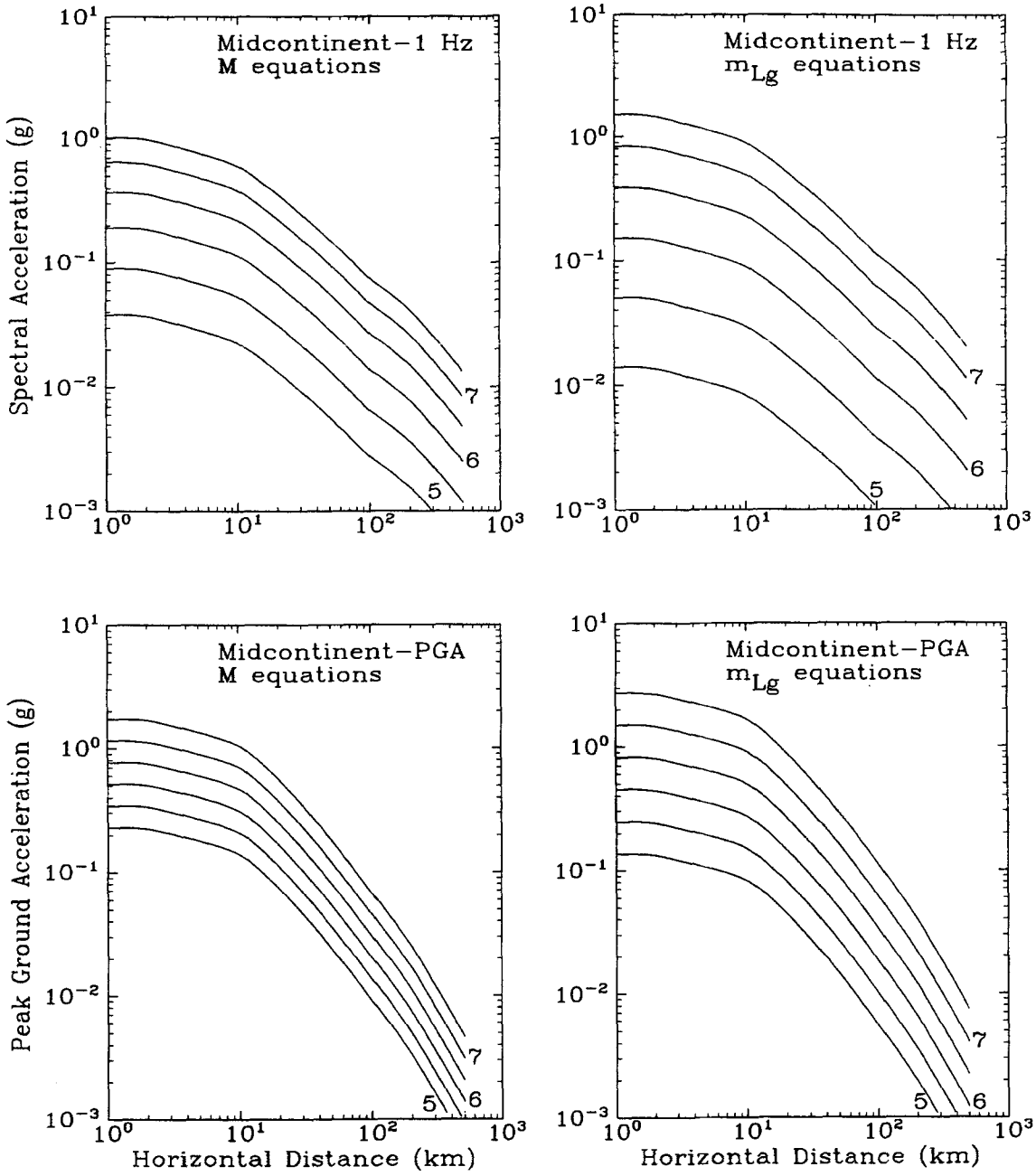

▲ **Figure 3.** Attenuation equations for the Mid-continent region; predictions for 1 Hz and PGA.

$$\sigma_a(M,R)=\sqrt{\sigma^2_{a,\text{modeling}+\Delta\sigma}(M)+\sigma^2_{a,depth+Q+\kappa}(R_{jb})} \qquad (5)$$

The magnitude-dependent aleatory uncertainty $\sigma_{a,\text{modeling}+\Delta\sigma}$ is approximated by three linear segments, defined by its values for three magnitudes (see Table 3). Values for other magnitudes are obtained by linear interpolation. The distance-dependent aleatory uncertainty $\sigma_{a,depth+Q+\kappa}$ is approximated as constant for R_{jb} < 5 km, varies linearly between 5 and 20 km, and is constant for R_{jb} > 20 km (see Table 4 for values at 5 and 20 km).

The epistemic uncertainty is magnitude-dependent (as was seen in Figure 6) and is approximated as a linear function of magnitude of the form:

$$\sigma_e(M)=\begin{cases}0.34+0.06(M-6) & M \text{ eqs, } f=0.5 \text{ Hz}\\ 0.36+0.07(M-6) & M \text{ eqs, } f\geq 1 \text{ Hz and PGA}\\ 0.37+0.10(m_{Lg}-6) & m_{Lg} \text{ eqs, } f=0.5 \text{ Hz}\\ 0.35+0.08(m_{Lg}-6) & m_{Lg} \text{ eqs, } f=1 \text{ Hz}\\ 0.34+0.07(m_{Lg}-6) & m_{Lg} \text{ eqs, } f\geq 2.5 \text{ Hz and PGA}\end{cases}$$

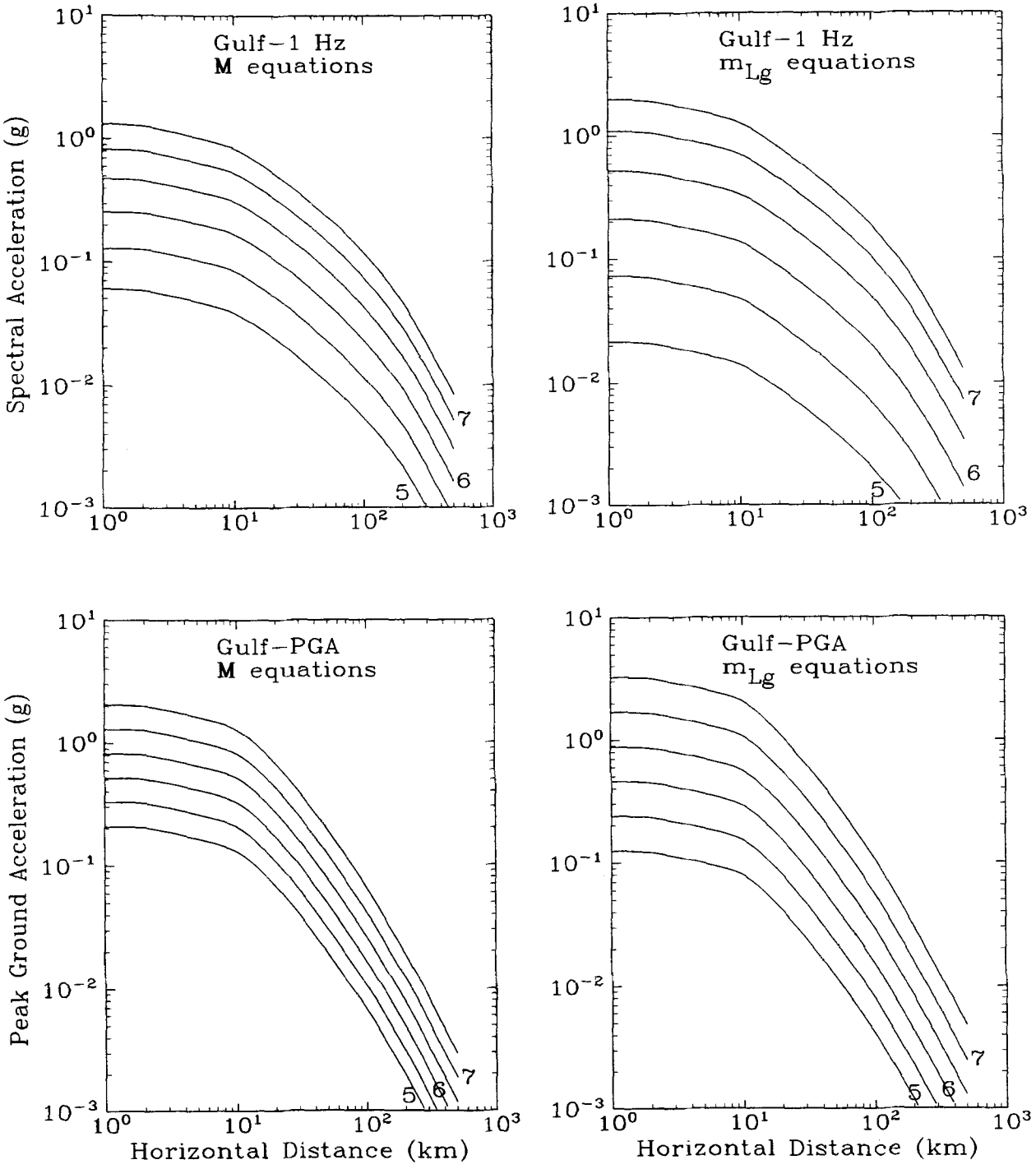

▲ **Figure 4.** Attenuation equations for the Gulf region; predictions for 1 Hz and PGA.

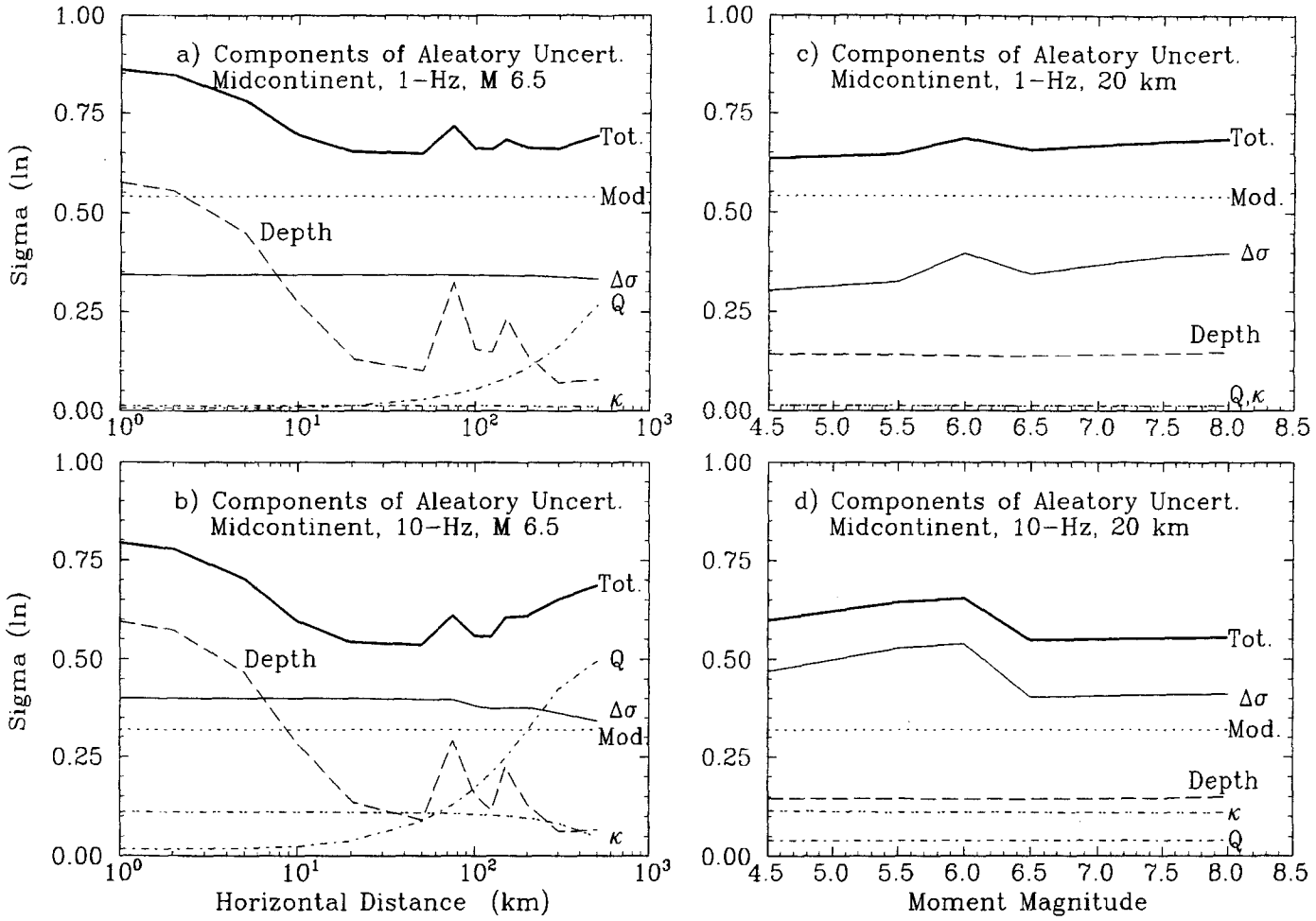

▲ **Figure 5.** Contributors to aleatory uncertainty in ground-motion predictions. Results shown as functions of both distance and magnitude.

TABLE 3
Values of Magnitude-Dependent Aleatory Uncertainty ($\sigma_{a,modeling+\Delta\sigma}$) for Critical Magnitudes

Freq (Hz)	M-based equations			m_{Lg}-based equations		
	***M* 5**	***M* 5.5**	***M* 8.0**	m_{Lg} 5	m_{Lg} 6	m_{Lg} 7.5
0.5	0.61	0.62	0.66	0.63	0.81	0.61
1.0	0.63	0.64	0.67	0.62	0.81	0.61
2.5	0.63	0.68	0.64	0.58	0.70	0.59
5.0	0.60	0.64	0.56	0.54	0.63	0.51
10.0	0.59	0.61	0.50	0.54	0.57	0.44
25.0	0.62	0.63	0.50	0.57	0.58	0.44
35.0	0.62	0.63	0.50	0.57	0.58	0.44
PGA	0.55	0.59	0.50	0.58	0.58	0.44

TABLE 4
Values of Distance-Dependent Aleatory Uncertainty ($\sigma_{a,depth+Q+\kappa}$) at Critical Distances

	Midcontinent		Gulf	
Freq. (Hz)	**<5 km**	**>20 km**	**<5 km**	**>20 km**
0.5	0.45	0.12	0.54	0.39
1.0	0.45	0.12	0.51	0.39
2.5	0.45	0.12	0.50	0.34
5.0	0.45	0.12	0.50	0.33
10.0	0.50	0.17	0.53	0.38
25.0	0.57	0.29	0.63	0.47
35.0	0.62	0.35	0.68	0.47
PGA	0.54	0.20	0.48	0.30

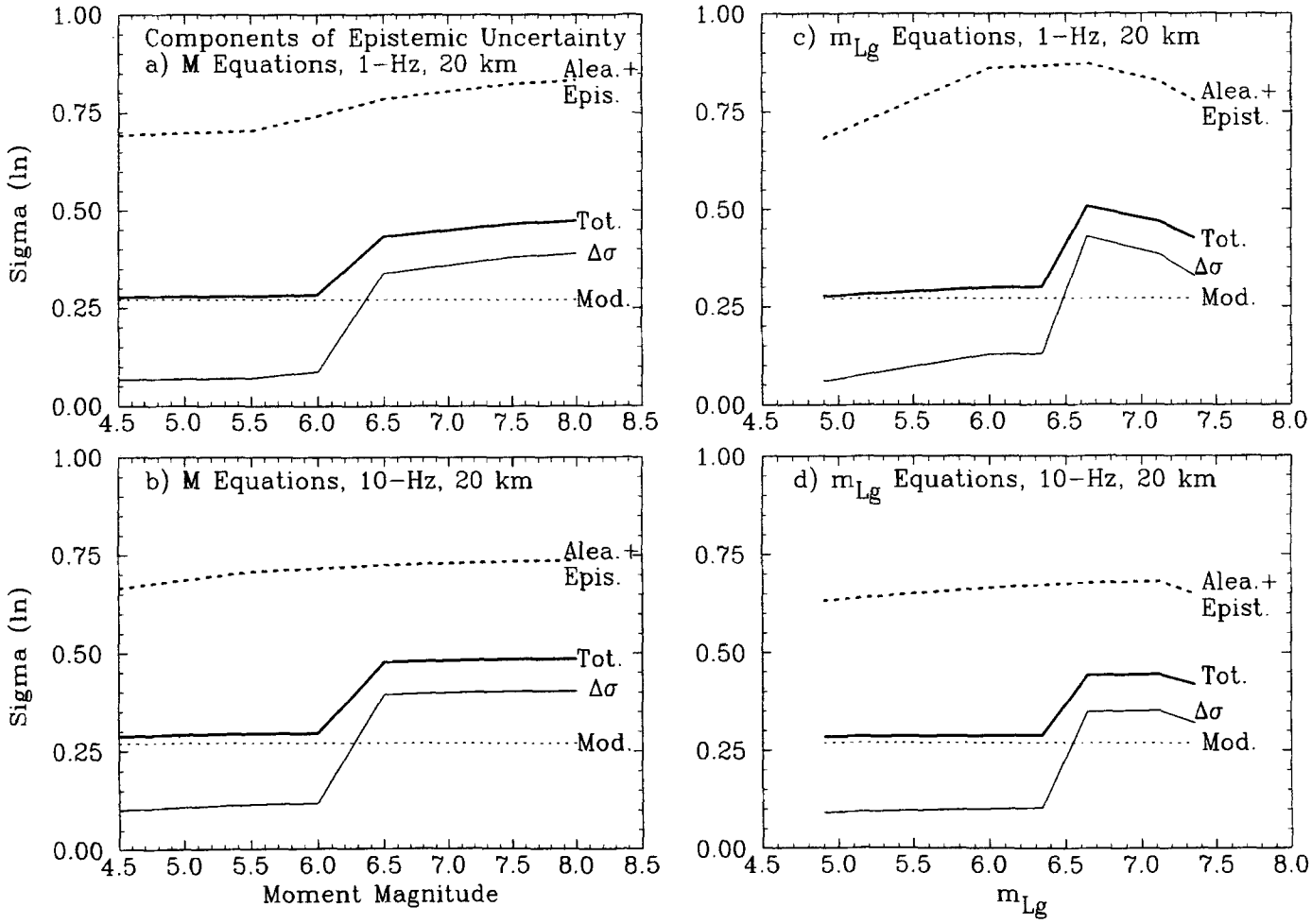

▲ **Figure 6.** Contributors to epistemic uncertainty in ground-motion prediction. Results shown for equations in terms of both *M* and m_{Lg}. Also shown is the total uncertainty.

DISCRETIZATION OF EPISTEMIC UNCERTAINTY FOR SEISMIC HAZARD ANALYSIS

In seismic hazard analysis, epistemic uncertainty is typically represented by considering multiple attenuation equations with weights related to their credibilities. This approach is natural when using attenuation equations developed by different authors or under a discrete set of alternative assumptions. This approach is also convenient because it lends itself to a logic-tree analysis and to the display of sensitivity. Aleatory uncertainty, on the other hand, is represented by a continuous random variable and is integrated over during the first step (*i.e.*, the conditional analysis step) of the seismic-hazard calculations.

The median predictions by the Engineering Model (represented by Equation 3 and Table 2) and the uncertainty represented by σ_e are transformed into a discrete set of attenuation equations. This is accomplished by replacing the normal distribution of the uncertainty term ε_e in Equation 3 with a discrete probability distribution. The discrete distribution consists of n values

$$\varepsilon_{e,i} = U_i \sigma_e(M), \quad i = 1, n$$

and their associated weights W_i, where U_i represents a value from a discrete approximation to a standard normal distribution. For $n = 4$, the values of U_i and W_i in Table 5 have been chosen so that the probabilistic moments up to order six of the four-point discrete distribution are equal to the corresponding moments of the standard normal distribution. By substituting Equations 7 and 6 in Equation 3 and using U_i values in Table 5, we obtain four alternative attenuation equations with associated weights. These alternative attenuation equations (which differ from the median attenuation equation in their C_1 and C_2 coefficients only) are given in Table 2, along with the median attenuation equations.

COMPARISON TO ENA GROUND-MOTION DATA

The CENA ground-motion data (see EPRI, 1993) are used for comparison to the Engineering ground-motion model developed here. In order to remove complications such as site effects and to limit the comparison to magnitudes and distances not too removed from the range of engineering interest, the following criteria are used for the selection of records for this comparison: (1) magnitudes $M \geq 4$, (2) distances less than 200 km, (3) horizontal components, (4) rock site conditions, (5) instruments located in shelters or at the lower level of buildings at most four stories high, and (6) estimate of stress drop available in Abrahamson *et al.* (1996a). Table 6 lists the records that meet these criteria. Figure 7 compares the observed spectral accelerations at 1 and 10 Hz to the predictions by the Engineering Model (using both the attenuation equations for M). The data are partitioned into two groups ($M \leq 5$ and $M > 5$). Predictions are shown as median curve, median $\times \exp(\pm\sigma_a)$, and median $\times \exp[\pm(\sigma_a^2+\sigma_e^2)^{1/2}]$. The reference magnitudes for the two groups of data are M 4.5 and 5.9, and m_{Lg} 5.0 and 6.5 (the reference magnitude for the large-magnitude group is chosen as the magnitude of the 1988 Saguenay earthquake). All observations are scaled to the corresponding reference magnitude. Figure 7 shows that the ground-motion amplitudes predicted by the Engineering Model are generally consistent with observations. The only discrepancy relates to the 1988 Saguenay earthquake. The observed 10-Hz amplitudes for Saguenay lay, on average, two standard deviations above the median (1.5 standard deviations for the m_{Lg} attenuation equations). This discrepancy is explained by the higher stress drop of this event. This stress drop is high, but is not inconsistent with the stress-drop distribution obtained in Abrahamson *et al.* (1996a). Additional comparisons to this dataset are contained in EPRI (1993) and Toro *et al.* (1996).

TABLE 5
Discrete Approximation to Standard Normal Distribution (Used to Discretize the Epistemic Uncertainty)

i	Distance U_i	Weight W_i
1	−2.33	0.046
2	−0.74	0.454
3	0.74	0.454
4	2.33	0.046

COMPARISON TO OTHER MODELS

Figure 8 compares the predictions by the Engineering Model for the Midcontinent region, in terms of both M and m_{Lg}, to predictions by other attenuation functions and ground-motion models for ENA. Predictions in terms of m_{Lg} are compared to predictions by the attenuation equations of Boore and Atkinson (1987) and McGuire *et al.* (1988; labeled EPRI, 1988). Predictions in terms of M are compared to predictions by the attenuation equations of Boore and Atkinson (1987) and Atkinson and Boore (1995).

The differences between predictions by the Engineering Model developed here and by the earlier attenuation equations are comparable to the uncertainties obtained in the previous section. This indicates general consistency between the new model and the earlier models. The differences at high frequencies are due to differences in ground-motion duration. The larger differences at low frequencies are due to the combined effect of duration and spectral shape. The only significant difference is with the Atkinson and Boore (1995) ground-motion model at 1 Hz and is due to differences in the assumed shape of the power spectrum of large earthquakes at low frequencies.

TABLE 6
Earthquake Records used in Comparisons

Event Name	Date	m_{Lg}	M	Site Name	R (km)	No. of Components	Code	Stress Drop (bars)
New Madrid, Mo	04/27/89	4.7	4.7	Old Appleton, Missouri	8.0	2	2	229
New Madrid, Mo	05/04/91	4.6	4.4	Old Appleton, Missouri	160	2	3	39
Saguenay, Can.	11/23/88	4.8	4.5	Dickey, Maine	198	2	4	53
New Brunswick (A)	03/31/82	4.8	4.0	Indian Brook II, N.B, (IB2)	0.8	2	1	96
New Brunswick (A)	03/31/82	4.8	4.0	Mitchell Lake Rd, N.B (ML, Temp.)	4.0	2	1	96
New Brunswick (A)	03/31/82	4.8	4.0	Hickey Lake, N.B, (HL, Temp.)	4.1	2	1	96
Nahanni, Can.	12/23/85	6.4	6.7	Nahanni, NWT, Station 2	7.4	2	5	86
Nahanni, Can.	12/23/85	6.4	6.7	Nahanni, NWT, Station 1	7.6	2	5	86
Nahanni, Can.	12/23/85	6.4	6.7	Nahanni, NWT, Station 3	22.6	2	5	86
Saguenay, Can.	11/25/88	6.5	5.9	GSC Site 17 - St-Andre-Du-Lac, Que	64.1	2	6	655
Saguenay, Can.	11/25/88	6.5	5.9	GSC Site 20 - Les Eboulements, Que	90.	2	6	655
Saguenay, Can.	11/25/88	6.5	5.9	GSC Site 8 - La Malbaie, Que	93.	2	6	655
Saguenay, Can.	11/25/88	6.5	5.9	GSC Site 14 - St. Lucie de Beaur., Que	101.	2	6	655
Saguenay, Can.	11/25/88	6.5	5.9	GSC Site 5 - Tadoussac, Que	113	1	6	655
Saguenay, Can.	11/25/88	6.5	5.9	GSC Site 10 - Riviere Quelle	118	2	6	655
Saguenay, Can.	11/25/88	6.5	5.9	GSC Site 1 - St. Ferreol, Que	117	2	6	655
Saguenay, Can.	11/25/88	6.5	5.9	GSC Site 9 - St. Pascal, Que	132	2	6	655
Saguenay, Can.	11/25/88	6.5	5.9	Dickey, Maine	197	2	6	655

GROUND-MOTION PREDICTIONS FOR SOIL SITES

Silva *et al.* (1996, see also EPRI, 1993) have calculated spectral acceleration and PGA amplification factors for five separate CENA soil categories and for various levels of shaking. Median ground-motion predictions for CENA soil sites are obtained by multiplying the spectral accelerations and PGA for rock, calculated using Equation 3 and Table 2, by the appropriate amplification factors from Silva *et al.* (1996).

Intuitively, the uncertainty in ground motion at soil sites would be estimated by adding the uncertainty in site response to the uncertainty in the input rock ground motion. The uncertainty in the input rock ground motion would be estimated by the uncertainty in the rock attenuation relation. Although intuitively appealing, this procedure would significantly overestimate the uncertainty in soil ground motions. In the discussion that follows, we show that the uncertainty in ground motions for a given soil site category is actually less than for rock sites. We recommend using the rock-site uncertainty as a conservative estimate of the soil-site uncertainty.

There are two main issues to consider in comparing the uncertainty of soil site and rock site ground motions. The first is the uncertainty in the site response for low to moderate levels of shaking and the second is the uncertainty in non-linear site response for high levels of shaking.

For low to moderate levels of shaking, the uncertainty in ground motion on soil and rock sites can be compared using recordings from dense arrays of seismometers. Abrahamson and Sykora (1993) examined the spatial correlation of response spectra using data from nine dense arrays. Five of the arrays were located on rock and four were located on soil. The amplitude variation for each array was fit to the functional form:

$$\sigma(f,\xi) = c_1(f,M)\left[1-\exp\left(c_2(f)\right)\right] \tag{8}$$

where σ is the standard deviation of the difference $\ln[Sa(f)]$ between two sites separated by a distance ξ, and $c_1(f,M)$, $c_2(f)$ are constants for each frequency and magnitude range that are estimated by maximum likelihood. The resulting response spectral variation models are shown in Figure 9. The uncertainty in ground response at rock sites is larger than or equal to the uncertainty at soil sites. The small-magnitude (M 4.1–4.7) rock-site standard deviation is larger than the small-magnitude (M 4.1–4.7) soil-site standard deviation at low and high frequencies, whereas the two are similar at intermediate frequencies (3–7 Hz). The large-magnitude rock-site curve comes from a single event (Coalinga aftershock) so it is not as robust as the other curves, but it also shows larger standard deviations than the M 5 soil-site curve for frequencies of 1 to 7 Hz.

If the total aleatory uncertainty in spectral acceleration at soil sites is computed by simply adding the variance in soil amplification to the variance in the rock spectral accelera-

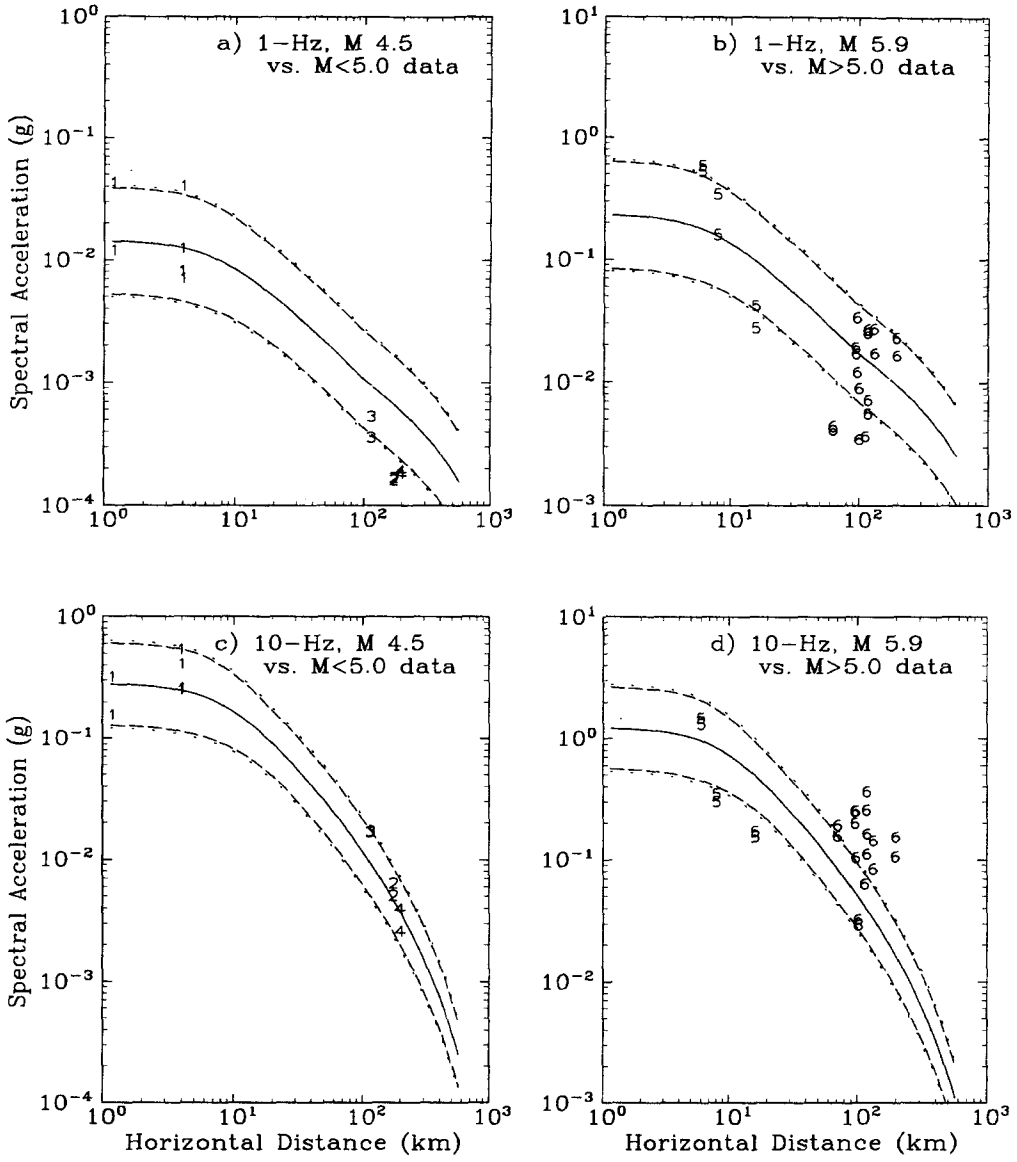

▲ **Figure 7.** Comparison of ground-motion predictions (in terms of *M*) to ENA data. Dashed lines: $\pm\sigma_{aleatory}$ bounds; dots: $\pm\sigma_{aleatory+epistemic}$ bounds. See Table 6 for earthquake symbols.

tion, then the uncertainty in spectral acceleration would be higher for soil sites than for rock sites. The dense-array data, however, suggest that the opposite is true. This suggests that either the soil has a homogenizing effect on ground motions or that the uncertainty in the bedrock motions is lower than the uncertainty in the outcrop motions.

A second concern is whether the uncertainty in the high-strain properties of soil sites should increase the total uncertainty of soil site ground motions for large ground motion levels. This issue was examined by modeling site response using a range of soil properties for site category 4 using the equivalent linear procedure described in Silva *et al.* (1996). The uncertainty in the resulting surface ground motion was computed for two sites from events with magnitudes ranging from 5.5 to 7.5. The results are shown in Figure 10. As the amplitude of shaking increases, the uncertainty in the ground motion decreases slightly. We conclude that the effect of nonlinear response is to reduce the uncertainty in surface ground motions such that it counteracts the additional uncertainty due to variations of the soil properties.

These results imply that the uncertainty computed for rock sites is an upper bound for the uncertainty on soil sites in a given site category. Therefore, we recommend using the uncertainty of ground motion given here for rock sites as a conservative estimate of the uncertainty of ground motion for soil sites.

DISCUSSION

The median attenuation equations and the associated models of aleatory and epistemic uncertainty presented here embody the ground motions predicted using the ground-

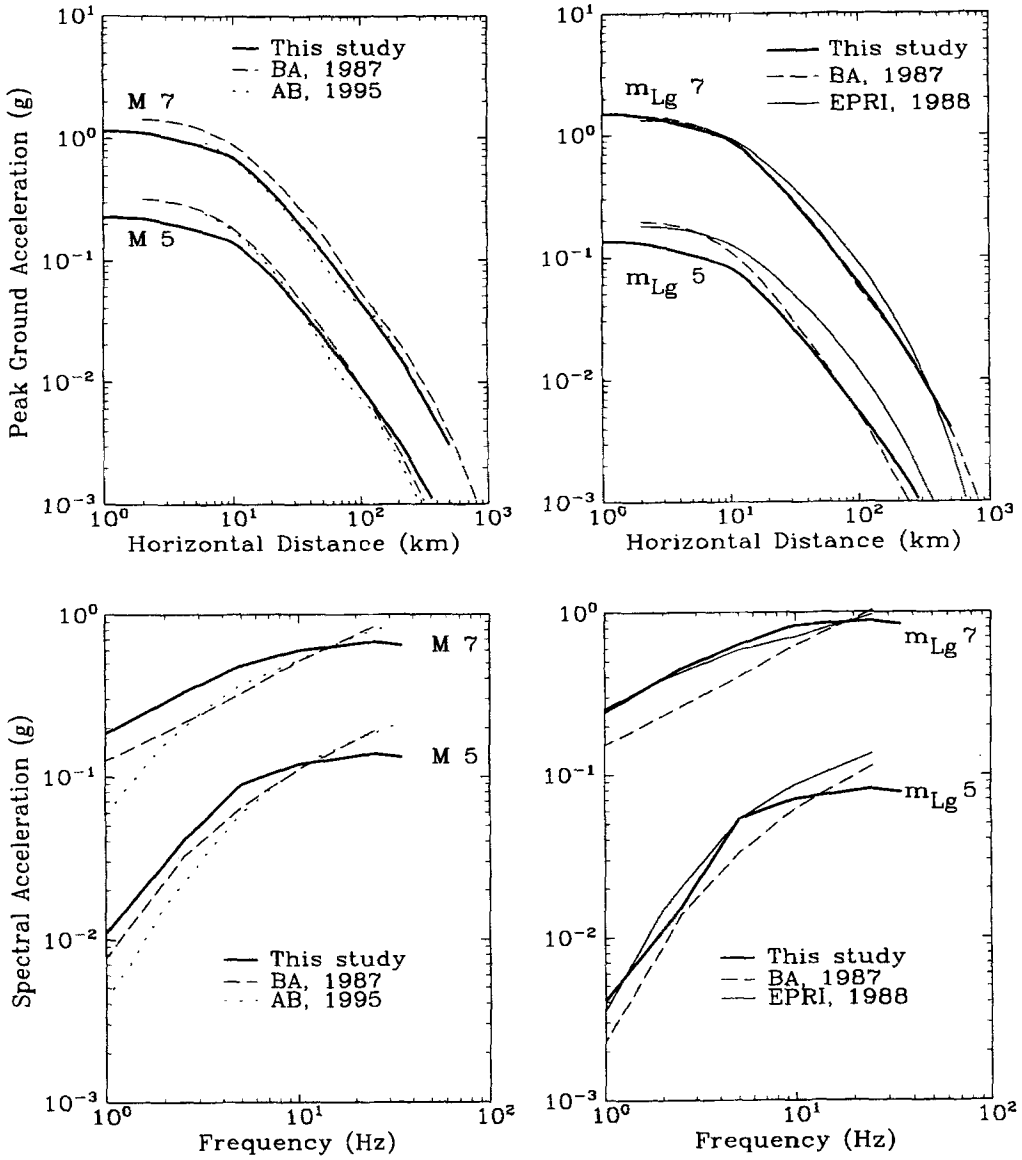

▲ **Figure 8.** Comparisons of ground-motion predictions for Midcontinent region to other attenuation equations for ENA.

motion models and parameters presented in EPRI (1993), Schneider *et al.* (1996), and Abrahamson *et al.* (1996a, 1996b). Though slightly more complicated than most attenuation equations in current use, these attenuation equations are in a form suitable for the determination of design ground motions and for seismic hazard evaluations.

Predicted ground motions for the Midcontinent and Gulf crustal regions are comparable to predictions by earlier models that use omega-square representations of the source spectra and are generally consistent with available records from CENA. The associated aleatory and epistemic uncertainties are similar to the values in current use for some cases (*i.e.*, high frequencies and moderate distances) and higher in other cases (*i.e.*, low frequencies or short distances). The high aleatory uncertainty at low frequencies is due to high modeling uncertainty (an additional contributor in the relations for m_{Lg} is uncertainty in the relationship between m_{Lg} and seismic moment; see Abrahamson *et al.*, 1996a). The higher uncertainty at shorter distances is due to the explicit consideration of aleatory uncertainty in focal depth.

What sets this study apart from the earlier studies of ground motions in CENA is the much larger amount of data that was collected and used to estimate model parameters, the more realistic modeling of crustal effects, and the rational, quantitative process used to derive the median predictions and associated uncertainties. These characteristics make the median predictions and measures of uncertainty presented here much more robust than earlier results.

It must be pointed out that these attenuation equations were derived using mainly point-source modeling assumptions (the only exception being the conversion of asperity depth to hypocentral depth, see EPRI, 1993). As a conse-

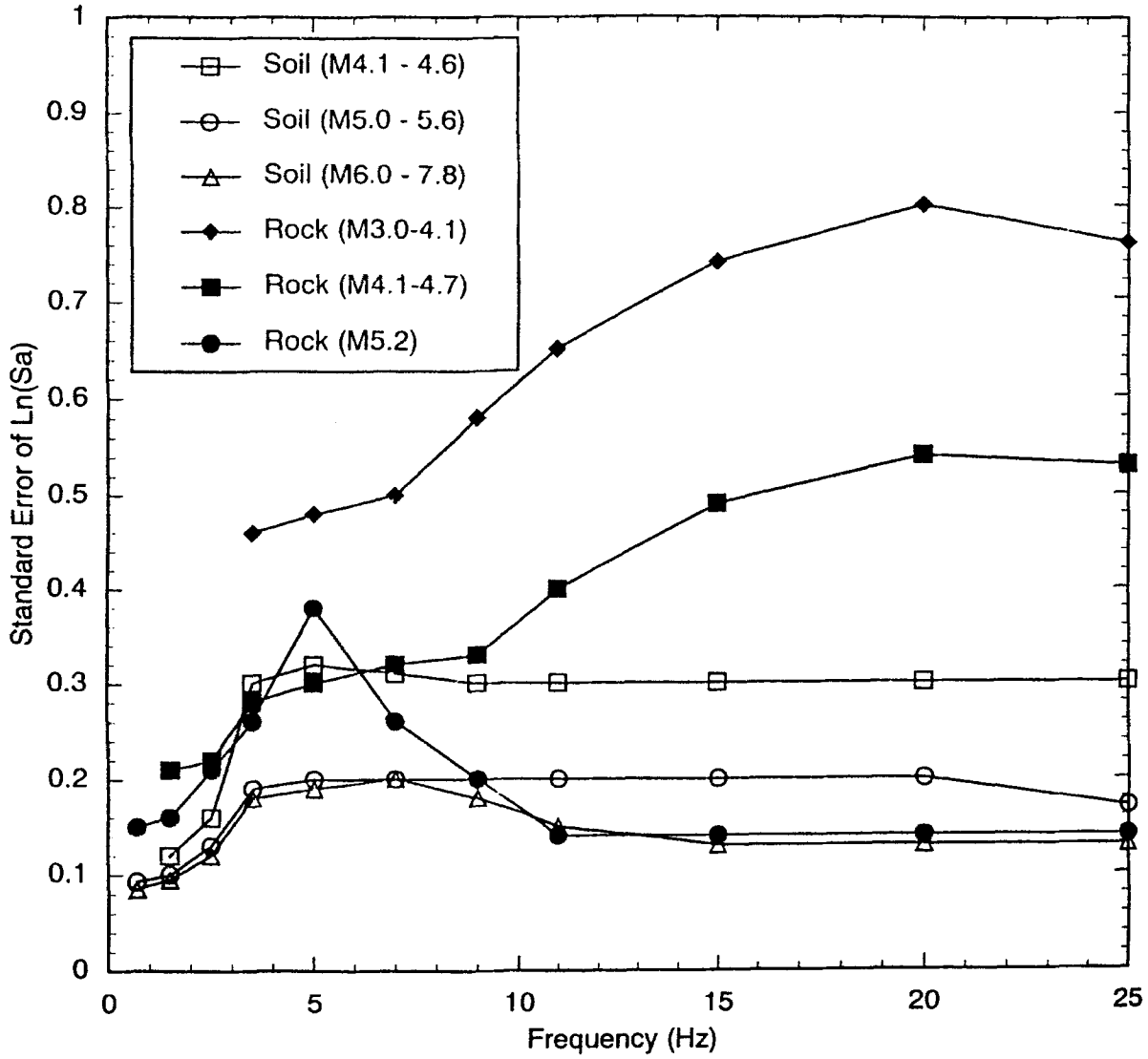

▲ **Figure 9.** Models of spatial variation of spectral acceleration as a function of frequency for a separation distance of 100 m. The open symbols are for soil sites and the solid symbols are for rock sites. Source: Abrahamson and Sykora (1993).

quence, these results may overestimate ground motions at sites near the rupture of a large earthquake because we have not included other geometric and potential source-scaling effects associated with extended ruptures. Therefore, caution should be exercised if these results are used to predict ground motions at distances shorter than one or two source dimensions. This limitation is of little significance for most sites in the Central and Eastern United States.

ACKNOWLEDGMENTS

This work was performed as part of the Early Site Permit Demonstration Project, under the direction of the EPRI, and sponsored by Southern Electric International, Commonwealth Research Corporation, Public Service Corporation of New Jersey, EPRI, the Nuclear Management and Research Council, the U.S. Department of Energy, and Sandia National Laboratories. We thank all project participants, particularly Gail Atkinson, Walt Silva, and Bob Youngs, for their inputs and comments.

REFERENCES

Abrahamson, N.A., P.G. Somerville, and C.A. Cornell (1990). Uncertainty in numerical strong motion predictions, *Proc. Fourth U.S. Nat. Conf. Earth. Eng.*, Palm Springs, CA, **1**, 407–416.

Abrahamson, N.A., and D. Sykora (1993). Variation of ground motion across individual sites., *Proc., Fourth DOE Natural Phenomena Hazards Mitigation Conference*, LLNL CONF-9310102.

Abrahamson, N.A., G.M. Atkinson, and G.R. Toro (1996a). Quantification of seismic source parameters for eastern North America, submitted to *Earthquake Spectra.*

Abrahamson, N.A., G.M. Atkinson, and G.R. Toro (1996b). Effect of the propagation path on ground motion in eastern North America, submitted to *Earthquake Spectra.*

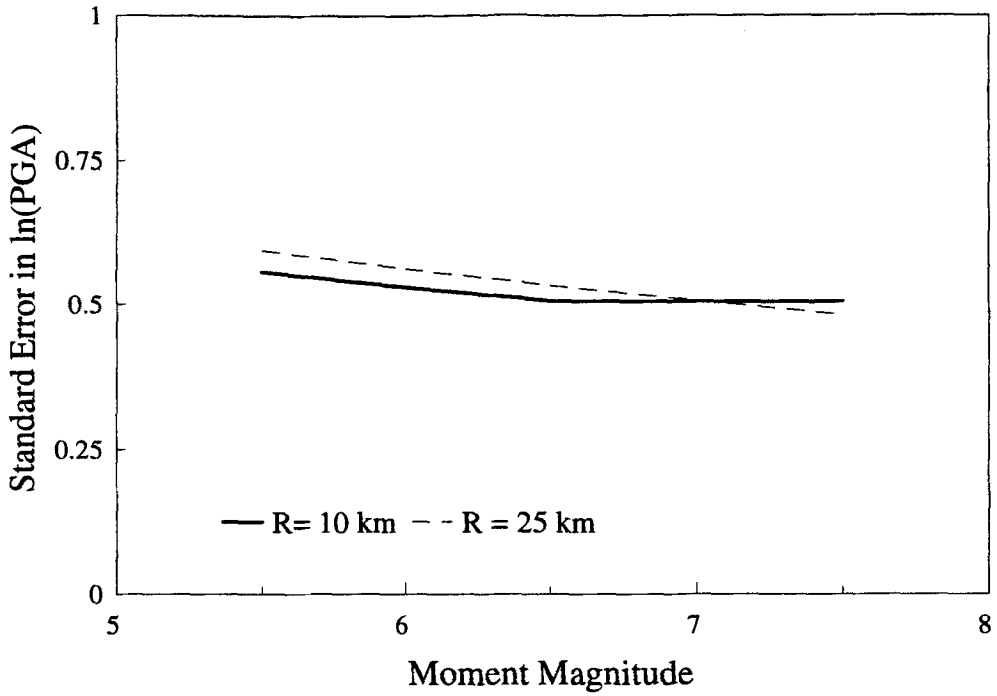

▲ **Figure 10**. Magnitude dependence of uncertainty in ground motion for two soil sites with 75 m depths to bedrock and horizontal distances of 10 and 25 km from the source. The computed uncertainty includes the effects of uncertainty in stress drop and in soil properties. The total uncertainty remains fairly constant as magnitude (and ground-motion amplitude) increases, even though the effect of site response becomes more important. After Silva *et al.* (1996).

Atkinson, G.M. (1984). Attenuation of strong ground motion in Canada from a random vibrations approach, *Bull. Seism. Soc. Am.*, **74**, 2,629–2,653.

Atkinson, G.M. (1993). Earthquake source spectra in eastern North America, *Bull. Seism. Soc. Am.*, **83**, 1,778–1,798.

Atkinson, G.M. and D.M. Boore (1995). Ground-motion relations for eastern North America, *Bull. Seism. Soc. Am.*, **85**, 17–30.

Boore, D.M., and G.M. Atkinson (1987). Stochastic prediction of ground motion and spectral response parameters at hard-rock sites in eastern North America, *Bull. Seism. Soc. Am.*, 77, 440–467.

Brune, J. (1970). Tectonic stress and the spectra of seismic shear waves from earthquakes, *J. Geophys. Res.*, **75**, 4,997–5,009.

Brune, J. (1971). Correction, *J. Geophys. Res.*, **76**, 5,002.

Electric Power Research Institute (EPRI) (1993). *Guidelines for Site Specific Ground Motions*, Palo Alto, California, Electric Power Research Institute, November, TR-102293.

McGuire, R.K., G.R. Toro, and W.J. Silva (1988). *Engineering Model of Earthquake Ground Motion for Eastern North America*, Palo Alto, California, Electric Power Research Institute, October, NP-6074.

Ou, G.B., and R.B. Herrmann (1990). A statistical model for ground motion produced by earthquakes at local and regional distances, *Bull. Seism. Soc. Am.*, **80**, 1,397–1,417.

Schneider, J.F., W.I. Silva, and P. Somerville (1996). Validation of ground motion models and modeling variability, submitted to *Earthquake Spectra*.

Silva, W.I., R. Pyke, R.R. Youngs, and I.M. Idriss (1996). Development of generic site amplification factors, submitted to *Earthquake Spectra*.

Toro, G.R., and R.K. McGuire (1987). An investigation into earthquake ground motion characteristics in eastern North America, *Bull. Seism. Soc. Am.*, 77, 467–489.

Toro, G.R., N.A. Abrahamson, and J.F. Schneider (1996). Engineering model of strong ground motions from earthquakes in the central and eastern United States, submitted to *Earthquake Spectra*.

Youngs, R.R., N.A. Abrahamson, F.I. Makdisi, and K. Sadigh (1995). Magnitude-dependent variance of peak ground acceleration, *Bull. Seism. Soc. Am.*, **85**, 1,161–1,176.

Risk Engineering, Inc.
4155 Darley Ave., Suite A
Boulder, CO 80303
(G.R.T.)

Pacific Gas and Electric Co.
245 Market St.
San Francisco, CA 94111
(N.A.A.)

Impact Forecasting, L.L.C.
230 W. Monroe Street
Chicago, IL 60606
(J.F.S.)